

Microsegregation In Autogenous Hastelloy X Welds

Analysis of solute segregation at fusion-zone subgrain and grain boundaries indicates that only sulfides and carbides are detrimental to hot-cracking resistance

BY W. F. SAVAGE AND B. M. KRANTZ

ABSTRACT. A previously reported investigation¹ at RPI developed and utilized a testing technique by means of which the hot-cracking sensitivity of sheet metal composite weld specimens may be evaluated. Bead-on-plate specimens were comprised of the microsegregation pattern characteristic of both the fusion-zone and heat-affected-zone. Accordingly, the augmented strain levels required to cause weld metal cracking at elevated temperatures were sufficient to evaluate both the relative cracking resistance of four laboratory heats of Hastelloy X and the effect on fusion-zone hot-cracking due to various residual S, Si, and Mn contents.

Optical microscopy revealed that microcracking was exclusively located at regions exhibiting segregation of solute. The presence of both etching effects and micron-size particles at subgrain- and grain-boundaries indirectly confirmed the hypothesis that the fusion-zone microsegregation resulted from the solidification process. Heat-affected zone microsegregation was believed to result from two phenomena: the solid-state reaction between the austenitic matrix and the numerous base-metal carbides, and the grain-coarsening process occurring immediately adjacent to the nominal fusion-zone boundary.

The present investigation involved studies of both the chemistry and the nature of the compounds located within these two regions displaying solute segregation. These studies were carried out by means of electron microprobe analyses of both fusion-zone subgrain-boundaries and microconstituents, and heat-affected zone carbides and carbide-matrix reaction prod-

ucts. To further elucidate the morphology of these microconstituents, specimen-current images with the electron microprobe were utilized. In addition, a comprehensive analysis of Debye-Scherrer powder patterns prepared from residues of electrolytically-dissolved weld metal provided the identification of a variety of fusion-zone compounds.

The specimen-current images of the weld metal microstructures confirmed the presence of solute-segregation at fusion-zone subgrain and grain boundaries. However, the thickness of each type of boundary as evidenced on the plane of polish was less than the resolution limit of the microprobe analyser; hence no direct identification of the solute species located at these boundaries was possible. The presence of several different types of compounds at sub-boundary triple points was conclusively indicated in several specimen-current image micrographs.

Analysis by means of the electron microprobe revealed these regions to be enriched significantly in Mo, S, and Si; moderately enriched in Cr and Mn; and depleted in Ni, Fe, and Co. The compounds detected by X-ray diffraction analysis of the weld metal residues included six sulfides, three carbides, two nitrides, and three miscellaneous constituents. Consideration of their respective physical properties and observed metallurgical behavior revealed that only the sulfides and carbides were detrimental to the hot-cracking resistance.

By means of specimen-current image microscopy, distinct regions of the heat-affected zone were observed to be enriched significantly in Cr, S and Si, although these regions were not detectable utilizing conventional optical techniques. These observations provided clear evidence of the heterogeneous distribution of solute and also the inadequacy of the usual metallographic techniques to detect all areas exhibiting microsegregation. Microprobe analysis of both the M_6C -carbides and the grain-boundary constituents formed from the reaction of these carbides and the matrix revealed enrichment in Mo, W, S, and Si generally, and a depletion in Ni, Fe, and Co when compared to the matrix analysis.

A literature survey of many investiga-

tions studying the problem of solute segregation resulting from solidification and the identification of segregated solute species in both iron-and nickel-base alloys is also included.

Introduction

A previous paper¹ has presented the results of a study of hot-cracking in Hastelloy X, a nickel-base superalloy. Developed during this earlier investigation was a novel testing procedure with which the hot-cracking propensity of four laboratory heats differing only in their respective S, Si, and Mn contents was determined. Briefly, this testing procedure consisted of a modified hot-ductility test utilizing a composite test specimen containing a longitudinal bead-on-plate gas tungsten-arc weld containing no added filler metal. The transverse cross section of the specimen was thus comprised of a full-penetration, autogenous fusion-zone bounded on both sides by actual weld heat-affected zones. Each specimen was then subjected to a synthetic weld thermal cycle and to predetermined levels of augmented strain at various preselected sub-solidus temperatures. In this manner, the effects of S, Si, and Mn on the hot-cracking resistance of the four laboratory heats of Hastelloy X was deduced by observing the levels of augmented strain required to induce fusion-zone microcracking. It was found that S significantly lowered the resistance to hot cracking when increased from 0.008 to 0.021 wt-%, and that both Si and Mn appeared to have beneficial effects when increased from 0.25 to 0.46% and from 0.31 to 0.93%, respectively.

Metallographic studies performed during the previous study conclusively demonstrated that hot-microcracking occurred exclusively in both the fusion-zone and heat-affected zone at highly localized regions exhibiting ex-

W. F. SAVAGE is Director of Welding Research, Dept. of Materials Engineering, Rensselaer Polytechnic Institute, Troy, N. Y., and B. M. KRANTZ, formerly a Graduate Assistant at Rensselaer Polytechnic Institute, is Manager, Metallurgical Development, Airco Welding Products Div., Air Reduction Co., Inc., Murray Hill, N. J.

Based on paper presented at the AWS National Fall Meeting held in St. Louis, Mo., during Oct. 3-6, 1966—also based on a thesis submitted by B. M. Krantz to the faculty of Rensselaer Polytechnic Institute in partial fulfillment of requirements for a PhD degree.

tensive microsegregation of solute. The segregation present in the weld metal was believed to result from the solidification process. On the other hand, that in the heat-affected zone apparently resulted from a series of complex solid-state reactions between the original matrix carbides and the austenitic matrix.

Several types of mechanisms causing solute segregation were tentatively identified. It was for the explicit purpose of identifying the nature of the segregating species and establishing their individual influence on hot-cracking that the latter portion of this investigation was undertaken. The following provides a review of the literature published through 1965 pertaining to solute segregation occurring in castings and both weld fusion-zone and weld heat-affected zone microstructures.

Solute Segregation

Solute Segregation Resulting from Solidification

Some investigators^{2,3} have attempted an analytical treatment of solute segregation during solidification. However, their studies have considered only the simple case of a slowly moving planar solid-liquid interface in high-purity alloys, rather than the rapid growth rates and complex alloy systems encountered in practical welding processes. Weinberg⁴ observed in a study of solute segregation in high purity Sn and Pb alloys that the ratio of the average solute concentration in the solidified dendrite to the average solute concentration in the remaining liquid was approximately 0.6% for nominal concentrations of several solute elements to a maximum of 1000 ppm. Therefore, the solidification process apparently resulted in approximately a 600% increase in solute concentration in the liquid phase.

The segregation ratio (defined as ratio of maximum to minimum solute concentration) was measured in a study⁵ of solute distribution in 0.4C-Ni-Cr steel castings. With the aid of an electron microprobe, a minimum solute concentration was observed at the center of dendrite stalks and a maximum at the interdendritic regions, resulting in segregation ratios of Mn and Cr of 1.6 and 1.2 respectively. Other investigators⁶ have evaluated the segregation ratio of Mn in 2-ton ingots of a low carbon Ni-Cr-Mo steel to be approximately 1.02 to 1.4.

Other work in the study of segregation in castings has evolved around the identification of the segregating species. In the iron-base superalloy A286

(1.95 Ti-0.25 Al-1.21 Mn-1.66 Mo-14.75 Cr-25 Ni-Bal. Fe), the "freckle" segregate frequently observed in consumable-electrode castings has been shown⁷⁻⁹ to result from the normal segregation of Ti, Si, and Mo. In fact the "freckles" have been eliminated⁷ by maintaining the Si content below 0.10%. In as-cast samples of SM-200 (9Cr-12.5W-1Cb-2 Ti-5 Al-10Co-Bal. Ni), Gregg and Pearcey¹⁰ have identified a grain-boundary constituent to be the Ni-Ni₃Al eutectic. In addition, Beattie and Ver Snyder¹¹ have shown that the M₆C carbide is present as a grain-boundary phase in the as-cast structure of alloy M252 containing 0.14 C, 1.09 Si, 1.22 Mn, 19.08 Cr, 10.04 Co, 10.69 Mo, 1.98 Ti, 0.35 Al, 3.39 Fe, and the balance Ni.

Many investigators have theorized or directly identified the specific elements partitioned to grain-boundaries or cell boundaries during weld metal solidification. Sulfur, for example, has been universally believed¹²⁻²² to promote hot-cracking in both Fe- and Ni-base alloys by the formation of low-melting interdendritic sulfides.

The presence of Si has also been generally regarded^{9, 12, 15, 21, 23-27} to be detrimental to the hot-cracking resistance of weld metal in both Fe- and Ni-base alloys. However, in a statistical study of individual elements, Hoerl and Moore¹⁶ considered Si to have only a minor effect on the cracking sensitivity of Type 347 stainless steel weld metal. In addition, Rozet¹⁸ has shown that, in an 15 Cr-35 Ni alloy, superior room temperature ductility is associated with an optimum silicon content. The influence of silicon in promoting cracking is unknown, but is thought to result from the formation of low-melting silicides, silicates, or eutectics.

The effect of Mn in weld metal has been generally acknowledged^{16, 19} to be beneficial by combining with S to form a relatively stable MnS. Otherwise it is believed that lower-melting sulfides form tending to promote hot-cracking. Zirconium often present as a residual deoxidant, has been reported^{15, 21, 28} to cause a detrimental increase in the incidence of hot-cracking. It has been hypothesized that low-melting zirconium compounds may form which promote cracking with zirconium contents varying from 0.25-0.75%. Studies²⁹ have shown Zr to promote surface liquation when unwelded specimens of Hastelloy X are rapidly heated, an observation suggesting its crack-promoting tendency.

The presence of oxygen is also believed to promote weld metal cracking, although no mechanism has been

proposed. However, it is probable that the presence of oxygen has a synergistic influence^{15, 30-32} on the contribution of other elements to hot-cracking.

In a comprehensive study of solute segregation in a modified SAE 4340 weld metal, Randall *et al.*¹⁷ observed the composition of the interdendritic regions to be increased relative to the matrix as follows: S increased 200-1700%, P increased 15-74%, Si increased 22 to 100%, Fe decreased 9-30% and Mo, Ni, and Cr essentially unchanged. For the Ni-base superalloy Udimet 700, Owczarski³³ reports enrichment of Ti, Mo, and Al within interdendritic areas and depletion of Cr, Co, and Ni. The detection of sigma phase and MC-carbides in grain boundaries also is indicative of solute segregation at these regions.

In a microprobe study of Type 310 stainless steel tensile specimens melted and cooled in such a manner as to synthesize the thermal history of weld metal, Cordea *et al.*³⁴ reported a small increase of Cr and depletion of both Ni and Fe at dendrite boundaries.

Other evidence of positive solute segregation during solidification is offered by the experimental observation of intergranular compounds formed as a result of solute segregation. These compounds are postulated to be either sulfides,^{13, 14} carbides,³⁵⁻³⁷ or other complex compounds.³⁴⁻³⁸ Other intermetallic compounds indicative of the presence of segregation at dendritic boundaries have been identified in steel weld metals, including: MnSiO₃, shown to be present at dendrite boundaries of a 0.5C-1.17 Mn steel,³⁹ Cr₇C₃ and MnS, identified on intergranular fracture surfaces of a steel containing 0.13C-4.0Ni-1 38Cr-0.49Mn-Bal. Fe,⁴⁰ and Fe₄Cb₅Si₃, observed in a 19Cr-3Ni-Cb stainless steel weld metal.²⁵

Carbides have been dominant constituents observed in the weld metal of Ni-base alloys. The M₆C-type carbide has been suggested⁴¹ as a likely possibility and has been identified along with CbC and Cr₇C₃ in the weld metal of Alloy-N155. Slaughter *et al.*⁴² indicate that carbides are also present at interdendritic areas in Hastelloy B welds, but no definite identification was reported. Other compounds detected include Ti(C, N) and CbC, identified in Inconel weld metal,⁴³ and both Cr₇C₃ and Fe₂Ti, detected in Inco 718 weld metal.⁴⁴ In short, the great variety of complex compounds observed at the dendritic boundaries in weld metal is indicative that significant solute segregation

must occur during the solidification of a weld.

Solute Segregation in Unmelted Base Metal

The chemistry of grain-boundaries in both metals and nonmetals and their effect on bulk properties is the subject of a review paper by Westbrook.⁴⁵ Among the many techniques reported by Westbrook for the detection of grain-boundary segregation are chemical analysis of intergranular fractures, tracer analysis using radioactive solute elements, and micro-hardness testing. Differences in the characteristic response to etching solutions sensitive to the presence of specific elements may also be used to detect areas of local inhomogeneity.

An interesting phenomenon of grain-boundary segregation observed in weld heat-affected zones^{1, 46} is that of "ghost" grain-boundaries.^{47, 48} The most common interpretation has been the inability of certain elements, originally segregated at grain-boundaries, to diffuse fast enough to follow the movement of the migrating grain-boundaries. Thus, a solute network remains outlining the prior grain-boundary network.

Along with the observation of variations in the mechanical and chemical properties of grain-boundaries, several investigators have succeeded in identifying the segregated solute species. Masubuchi and Martin⁴⁹ observed positive segregation of both Si and S extending a distance 3-4 grain diameters from the fusion-zone into the heat-affected zone boundaries of HY-80 steel weldments. In a medium carbon steel, Boniszewski and Baker³⁹ studied the dissolution behavior of MnS in heat-affected-zone boundaries. Exposure to temperatures greater than 1250° C (2282° F) caused dissolution of the MnS. In the same study the authors report the tentative identification of CaS at heat-affected zone grain-boundaries. Further study of the behavior of MnS by Brammar⁵⁰ has shown that MnS reprecipitates in a fern-shaped (dendritic) fashion after liquation and that grain-boundary sulfides may also contain Cr and Fe as part of the metallic radical. In addition, FeP was also observed to be precipitated within heat-affected zone grain-boundaries.

In a study of grain-boundary sulfide chemistry, Brammar and Honeycombe⁵¹ report that Cr-rich sulfides form in preference to MnS in a high-purity experimental Fe-base alloy containing 0.16S-0.24Mn-1.64Cr. The addition of 0.4% Ni caused no change in sulfide composition. These results were confirmed by electron micro-

probe examination of the sulfides.

Confirmation of these results is reported by Kiessling and Lange,⁵² who indicate that the solubility of Cr in MnS at 950° C (1742° F) and 1250° C (2282° F) is 70 atomic-% of the metal atoms. On the other hand, the corresponding solubility of Mn in Cr₇S₈ is much smaller. In response to the above discussion⁵² Brammar and Honeycombe⁵³ indicate that the metallic components of the sulfides observed are mainly Cr with traces of Fe and Mn if the Cr/Mn ratio exceeds 12. On the other hand, if this ratio does not exceed 7, Mn becomes the major metallic component of the sulfide.

The studies reported above have been confirmed and extended by continued investigation by Kiessling and Westerman of the chemistry of MnS-type sulfides.⁵⁴ These authors report that 65% of the Mn atoms are replaced by Fe or Cr atoms at 1150° C (2072° F) at the solubility limit thus corroborating the previous data as noted above. The entire series of the first period transition metals display varied degrees of solid solubility in (Mn, Me) S-type sulfides, e.g., Co and Ni replace 28 and 12% of the metal atoms, respectively. Thus a complex pattern of metal sulfides may well exist and in fact do exist in varied proportions in the same alloy.

In a study of austenitic welds, Topopov⁵⁵ suggested the presence of grain-boundary carbides as a result of micro-hardness data and metallographic observation. He also postulated that Fe₃C may have a significant solubility for S and thus form a ternary Fe-Fe₃C-FeS eutectic. Another study⁵⁶ of austenitic Fe-base alloys has led to the proposal that the cause of grain-boundary liquation in low C-high Cb Type 347 stainless steel is a eutectic mixture of Cb carbides and nitrides with minor amounts of Mn, Si, and Fe also present. A heat-affected zone eutectic constituent in the Ni-Mo alloy, Hastelloy N, was positively identified⁵⁷ to be an M₆C-type carbide.

Underlying the concern regarding the existence of heat-affected zone microsegregation is the logical assumption that these solute-rich regions behave like a separate alloy system in response to the welding process. In support of this belief is a study by Stickler and Vinckier⁵⁸ who report that the (Fe, Cr)₂₃C₆ carbide precipitating in the grain-boundaries of Type 302 stainless steel does not nucleate from the matrix, but rather grows from within the grain-boundary as a series of large thin dendrites.

The importance of intergranular

constituents is also shown in the work of Smith and Spencer⁵⁹ who indicate that the grain growth of pure Ni saturated with NiS is a surface-diffusion-controlled process. Additional evidence is offered in the work of Cordea *et al.*³⁴ who indicate that an increase in grain size in Inconel as a result of exposure to elevated temperature is accompanied by a simultaneous loss in hot-ductility.

A novel cracking mechanism, proposed at RPI and first investigated by Dudley,⁶⁰ predicts the formation of a liquid film at sub-solidus temperatures as a result of the nonequilibrium conditions prevailing in the weld heat-affected zone. Dudley showed that carbides in Type 347 stainless steel do undergo a liquation reaction at temperatures below the normal solidus during rapid heating and cooling, but was unable to demonstrate conclusively that a eutectic reaction with the surrounding matrix occurred.

A subsequent investigation by Aronson⁶¹ of the same phenomenon in a 1% carbon high-carbon steel showed that the Fe-C eutectic could form in the presence of graphite at temperatures below the solidus of the matrix. However, Fe-Fe₃C eutectic melting was not produced by rapid heating of the same alloy when all of the carbon was in the combined form. Presumably this is a result of the thermodynamic instability of the cementite phase above the A₁ temperature. However, Owczarski *et al.*⁶² and Sullivan⁶³ extensively studied this phenomenon, termed "constitutional liquation", in the heat-affected zone of Udimet 700 and other superalloys. In doing so, they observed a lamellar liquation product believed to be the reaction product of MC-type carbides and the matrix to produce melting at a temperature well below the expected solidus for the nominal composition of the alloy. This latter work has recently been summarized⁶⁴ in a paper redefining the weld-heat-affected zone to account for the various nonequilibrium processes occurring.

Subsequent to the completion of the present investigation, Savage and Pepe⁶⁵ studied the kinetics of formation and dissolution of liquid-like grain-boundary constituents in an 18-Ni maraging steel. Extensive metallographic work conclusively showed that these constituents were formed by the partial decomposition of TiS compounds in accordance with the constitutional-liquation hypothesis.

Material

The four heats of Hastelloy X studied during this phase of the investigation were induction-melted under

argon, teemed into a transfer ladle, and poured into graphite molds using additions of an exothermic compound to prevent piping during the solidification process. The ingots were subsequently forged and hot-rolled at 2150° F to 1/16 in. sheet.

Table 1 contains the complete chemical analysis for each of the four heats studied. Each heat was assigned a two-letter code symbol, and for convenience the major distinguishing features of each heat are summarized below:

1. Heat MG—low S (0.008%), moderate Si (0.46%), low Mn (0.31%).
2. Heat MJ—low S (0.008%), low Si (0.29%), high Mn (0.86%).
3. Heat MK—high S (0.021%), low Si (0.29%), high Mn (0.93%).
4. Heat ML—low S (0.011%), low Si (0.25%), low Mn (0.31%).

Experimental Procedure

Identification of Heat-Affected Zone and Weld-Metal Constituents

A previous paper¹ by the present authors presented metallographic evidence defining the intimate relationship between hot-cracking and solute-segregation. They also presented the results of the hot-cracking test evaluating the effect on hot-cracking due to varied concentrations of three selected alloy elements. Consideration of these results indicated a strong need both to identify the solute elements segregated in the weld-metal and the heat-affected zone, and to establish their state of combination since the localized properties of the grain- and

subgrain-boundary constituents undoubtedly govern the resistance to hot-cracking. Accordingly, a combination of electron microprobe X-ray diffraction and X-ray fluorescence analyses of weld-metal residues was performed to establish the chemical identity of the solute-rich regions.

The following electron microprobe analyses were performed by personnel of the Union Carbide Corporation, Mining and Metals Division, Niagara Falls, N.Y. on three selected composite weld specimens:

1. A determination of the composition of the microconstituents observed at the fusion-zone subgrain-boundaries in a sample of heat ML strained 16% at 2150° F.
2. A comparison of the extent of solute segregation within heats MK (high sulfur, low silicon, high manganese) and ML (low sulfur, low silicon, low manganese).
3. An investigation of the grain-boundary microconstituents observed in the heat-affected zone of a specimen of heat MK strained 14% at 2150° F.
4. An investigation of the heat-affected zone carbides and the reaction between these carbides and the surrounding matrix.

After marking pertinent polished and etched metallographic specimens with microhardness indentations to facilitate location of specific regions during the microprobe analysis, the samples were repolished with 0.03μ Linde B powder to remove all vestiges of the etching operation. The specimens were then cut to fit the specimen holder of the Associated Electronic

Industries Microprobe, mounted in a Woods Metal casting, and repolished prior to analysis.

The analyses of the concentrations of S, Si, and Mn in several cases were obtained by means of pulse counts, i.e., by recording the number of pulses of fluorescent radiation produced by each element during a fixed time interval. The chief problem encountered was the error involved in counting low pulse rates against a background of comparable magnitude. The most probable error in counting N pulses in a given time against a background of N_b counts is given by the following expression:⁶⁶

$$E = \frac{67(N + N_b)}{N - N_b} \text{ percent}$$

where: E = most probable percentage error, N = counts detected in a fixed time interval, and N_b = background counts detected during the same time interval.

The above equation may be applied as follows: Assume that 50 counts are detected and the existing background recorded is 4 counts over the same interval of time. The most probable error is therefore $67(54/46) = 10.17\%$ or 5.85 counts. Then the probability is 0.5 that the observed count of 50 lies within the range $N_t \pm 5.85$ counts where N_t is the true number of counts.

The most probable error is thus a measure of the precision of measurement. This value was then converted to weight percentage and presented for each analysis deduced by this pulse counting technique. The results should therefore be interpreted in light of the above argument.

Electrolytic Separation of Weld-Metal Microconstituents

The microconstituents observed in the weld metal of the four materials were separated for subsequent X-ray analysis by electrolytically dissolving the weld metal in a 20% aqueous solution orthophosphoric acid (H_3PO_4) found by other investigators⁶⁷ to be satisfactory for separation of minor constituents in nickel-base alloys. The base metal had been previously machined from as-welded composite test specimens leaving strips consisting only of weld-metal for dissolution. These strips were then ground on a 60X wet grinding belt, washed in water, pickled in aqua regia, rewashed in distilled water, and dried in reagent-grade ethyl alcohol to minimize the presence of any surface oxides or contaminants.

The strips were then connected to the positive terminal of a variable-

Table 1—Composition of Hastelloy X Heats Studied, Wt-%^a

Rensselaer code Stellite heat No.	MG	MJ	MK	ML	Range of 50 production heats
S	0.008	0.008	0.021	0.011	0.007– 0.021
Si	0.46	0.29	0.29	0.25	0.55 – 0.90
Mn	0.31	0.86	0.93	0.31	0.40 – 0.55
Cr	22.25	21.42	22.21	21.88	21.25 – 22.40
W	0.48	0.44	0.47	0.42	0.50 – 0.90
Fe	17.80	18.78	18.16	17.96	18.00 – 19.00
C	0.11	0.10	0.10	0.11	0.05 – 0.15
Co	1.38	1.38	1.36	1.48	0.75 – 1.60
Mo	8.79	8.72	8.80	8.80	8.70 – 9.20
P	LAP	LAP	LAP	LAP	0.015– 0.025
Zr	0.13	0.13	0.09	0.15	0.043– 0.11
Pb	0.001	0.001	0.001	0.001	Unknown
Cu	0.03	0.04	0.03	0.05	0.03 – 0.05
H ₂	6 ppm	6 ppm	7 ppm	4 ppm	N.A. ^b
O ₂	50 ppm	66 ppm	55 ppm	50 ppm	N.A. ^b
N ₂	772 ppm	770 ppm	906 ppm	454 ppm	300 – 400 ppm
Ni	48.05	48.42	47.17	Balance (48.46) ^c	Balance (49.69 – 45.0) ^c

^a The analyses and normal composition range of production heats were supplied by the Stellite Division (Kokomo, Indiana), presently a division of the Cabot Corporation.

^b N.A.—not available.

^c Obtained by subtraction.

voltage d-c power supply and immersed in the acid electrolyte, using a stainless steel sheet as a cathode. The all-weld metal specimen was then dissolved at a potential of 4-6 volts d-c, using an initial current density of 0.5-1.0 amp/in². When the specimen was completely dissolved, the electrolyte solution was decanted, the residue was centrifuged, then washed with distilled water and dried with ethanol.

X-Ray Analysis of Weld Metal Residue

The residues electrolytically separated from the weld metal were analyzed quantitatively using a 57.3 mm dia. Straumanis-type Debye-Scherrer powder camera. Glass fibers (0.0025 in. diameter) were coated with a thin layer of "Lubriscal" grease and then carefully rolled in the residue to form an extremely small-diameter cylindrical powder specimen. These specimens were critically centered in the camera specimen holder and rotated continuously throughout a 15 hr exposure using Ni-filtered CuK α radiation obtained from a Cu target tube operated at 35 kv and 15 ma. The grease used to coat the fibers was known⁶⁸ to display low intensity diffraction lines corresponding to "d" spacings of 4.10 Å (weak) and 3.75 Å (very, very weak). These lines were universally observed and were disregarded in analysis of the films obtained from the weld metal residues.

Film measurements were made with the aid of a commercially available⁶⁹ transparent scale calibrated in "d" spacings for the specific camera radius and radiation used. A test diffraction pattern obtained from 20 μ pure annealed tungsten powder was analyzed using the same X-ray techniques to verify the accuracy of the transparent scale and the procedure being used. The intensities of detected lines relative to the most intense were estimated visually in order to permit application of the Hanawalt identification procedure.

In general, procedure involves matching both the observed "d" spacings and the relative intensities of each diffraction line with similar data catalogued in the ASTM Powder Data File. All of the intense lines of a given compound must be detected in the proper order of intensity for a positive identification, since there can be no interference or cancellation of diffracted radiation. Since diffraction from a mixture is an additive process and each of the phases present produces its individual diffraction pattern independently of all others present, the analysis of a mixture of phases is much more difficult than analysis of a single phase.

This results from the fact that when two or more phases possess families of planes with the same "d" spacing the diffraction lines superimpose and the resulting line intensity is equal to the sum of the intensity of the radiation diffracted by each contributing phase. Thus, unless all possible superpositions are considered, the observed relative intensities may differ significantly from the catalogued relative intensities and make positive identification of the phases impossible. A trial-and-error method of solution to such a problem is discussed below.

The procedure used in analyzing the powder patterns will be illustrated with the aid of the data in Table 2, which presents a portion of the actual data obtained from the weld metal residue of heat MG.

Presented in the two left-hand columns of Table 2 are several experimentally observed "d" spacings and their relative intensities as estimated on a scale increasing from 0 to 100. The data in the columns headed by the three compounds, (M₆C, ZrN, and Ni₂Si) contain several "d" spacings and in subscript notation the catalogued intensity of each line relative to a rating of 100 for the strongest line of the particular compound. Thus the data available for the M₆C carbide observed in Hastelloy X indicate that the most intense diffraction line obtainable from a sample of only M₆C carbide corresponds to a "d" spacing of 2.10 Å, and is accordingly assigned a relative intensity of 100. Included in a complete pattern of this compound are additional lines corresponding to "d" spacings of 2.23, 2.51, and 2.74 Å, displaying relative intensities of 80, 20, and 10, respectively.

Similar series of lines with characteristic relative intensities are catalogued for each compound present and must contribute to the overall diffraction pattern. Such data, obtained from the ASTM Powder Data File, are also presented in Table 2 for both ZrN and Ni₂Si. For a diffraction sample containing these compounds the previously discussed superposition of lines can be expected at "d" values of 2.73, 2.27, and 2.10 Å.

As a starting point, the visually-assigned relative intensities are considered as absolute units of intensity. The apparent line intensity of each line was then compared with the catalogued line intensities for each possible compound with a corresponding "d" value. If the relative intensities of the observed lines for a particular compound did not agree with the catalogued values for the corresponding lines, it was necessary to assume that

superposition was contributing to the intensity of one or more lines.

For example, five lines on the pattern correspond to the position of the 3.31, 2.86, 2.73, 2.28 and 2.12 Å "d" spacings for Ni₂Si, but the apparent intensities failed to agree with the catalogued values. Thus, the intensity ratio $I_{2.86}/I_{2.12}$ should have been approximately equal to 1 if Ni₂Si were solely responsible. However, the observed ratio $I_{2.86}/I_{2.12} \cong 5/100 \cong 1/20$. Thus, it was obvious that superposition of a line from another more prevalent compound must have reinforced the 2.12 Å line. From Table 2, it can be seen that the 2.10 Å line for M₆C is a likely candidate. By the same reasoning the observed relative intensity of 40 exhibited by the 2.27 Å line could not be explained by the presence of either M₆C or Ni₂Si. Note that M₆C exhibits no line for this "d" spacing, while the observed $I_{2.28}/I_{2.86}$ ratio of $40/5 = 8$ could not be justified by the catalogued value of $100/60 = 1.6$. Thus it was necessary to assume the presence of ZrN with a strong line corresponding to 2.24 Å. By such trial-and-error reasoning, it was possible with the aid of the ASTM Powder Data File and a knowledge of the elements present to identify a combination of compounds which would tentatively explain all but two of the 50 lines present in each diffraction pattern.

The next problem was to assign an approximate "contribution factor" for each of the tentatively identified compounds in an effort to rationalize the observed ratios of line intensities. Again, this was done by trial-and-error and the product of the catalogued relative intensity and the contribution factors finally chosen is indicated in the form of a superscript at the right of each value of "d" spacing. Thus, for example, consider the case of the apparent relative intensities of the lines corresponding to "d" spacings of 2.27 and 2.62 Å with $I_{2.27}/I_{2.62} \cong 40/30 \cong 1.33$. By assuming contribution factors of 0.8, 0.3, and 0.05 for M₆C, ZrN and Ni₂Si respectively, and multiplying by the corresponding catalogued intensities, the intensity contribution of each compound to the observed pattern could be evaluated. Thus, for the 2.62 line, the ZrN contribution would be $0.3(100) = 30$ while M₆C and Ni₂Si contribute nothing. This figure for the "expected" intensity compares with the assigned value of 30. Similarly, for the 2.27 line the ZrN contribution would be $0.3(100) = 30$, that of the Ni₂Si would be $0.05(100) = 5$, while the M₆C contributes nothing. The expected intensity of $30 + 5 = 35$

compares reasonably well with the observed value of 40, and would predict $I_{2.27}/I_{2.62} \cong 35/30 \cong 1.16$ as compared with the observed 1.33.

This trial-and-error procedure was continued until the observed intensity ratios were justified within reasonable limits by the calculated values of the "expected" intensities.

The technique used in solving the diffraction patterns utilized the Mathews Co-ordinate Index, jointly published by ASTM and Jonker Business Machines, Inc. This index allows rapid screening of approximately 7700 inorganic compounds by utilizing a technique imposing certain conditions which must be satisfied by all possible solutions. For example, imposing both the "Positive Sulfur" and the "Negative Halogen" requirements automatically demands the presence of S and absence of any halogen element in the compounds identified.

Utilizing the results of the reported compositions of the four heats studied, electron microprobe analyses, and subsequent X-ray fluorescence analysis, the conditions listed below were imposed upon the searching system:

1. All compounds with any of their eight most intense lines corresponding to a "d" spacing greater than 7.00 Å were assumed to be absent.

2. All hydrates were assumed to be absent.

3. All of the following elements were assumed to be absent (grouped in accordance with Mathews Index):

- (a) Au, Tc, Pt, Ir, Ru, Rh, Os, Pd, Cu, Ag, Re.
- (b) B, Al, Ga, In, Tl.
- (c) Be, Mg.

- (d) F, Cl, Br, I.
- (e) Li, Cs, Rb, K, Na
- (f) Rare Earths, Sc.
- (g) V, Nb, Ta.
- (h) Zn, Cd, Hg.
- (i) Miscellaneous elements.

The results obtained are, of course, limited to the accuracy of these restrictions, and the availability of a complete accurate catalogue of all possible compounds.

As a further check of the chemical species present, X-ray fluorescence analysis was performed using the entire sample of each weld metal residue to obtain a qualitative chemical analysis. This study was carried out by personnel of the Analytical Services Laboratory, Silicone Products Dept., General Electric Company, Waterford, N. Y.

The residues were mixed with a small quantity of Testor's Household Cement, smeared into a thin layer on a Teflon specimen block, and mounted within the helium-filled specimen holder. Tungsten radiation at 50 kvp and 54 ma was used to cause fluorescence of the sample, although Cr radiation was also used to establish the unambiguous presence of W in the sample. Prior to analyzing the residues, a blank scan was made of both the cement and Teflon specimen support to eliminate the possibility of erroneous indications contributed by the chemistry of these two items.

Results and Discussion

Electron-Microprobe Analysis of Fusion-Zone Microconstituents

Figure 1 shows a specimen current image micrograph, taken at X1250, of the fusion-zone microstructure of a specimen from heat ML. The original

composite weld specimen was subjected to 16% strain at a testing temperature of 2150° F. The horizontal line A-A in Fig. 2 represents the locus of the microprobe traverses used in analyzing the individual microconstituents, and was selected such that the electron beam would intercept a typical subgrain-boundary and microconstituent located within such a boundary.

In general, a localized increase in the density of such an image recorded by monitoring the specimen current during the sweep of the electron beam is indicative of a localized increase in the concentration of atomic species of higher atomic number. This increase in density results from the fact that the absorption of electrons increases in efficiency with decrease in the atomic number of the element bombarded by the electron beam. Thus, regions rich in elements of high atomic number such as Cr, Mn, Fe, Co, Ni, Zr, Mo and W would tend to be darker in a specimen current image than regions rich in elements such as S, P, and Si with low atomic numbers. Of course, the reverse is true in an image produced by recording electron back-scatter. For ease of identification, the significant regions along the traverse are numbered in the schematic drawing comprising Fig. 2.

Table 3 summarizes the results of the microprobe analysis of the regions identified in Fig. 2 and shown in Fig. 1. The analytical data for Ni, Fe, Mo and Co were obtained from X-ray line scans, while those for Cr, S, Si and Mn were obtained by pulse counting

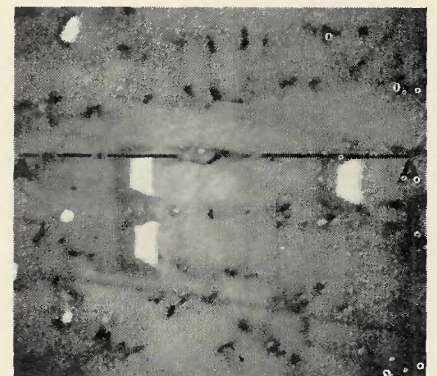


Fig. 1—Specimen current image of specimen of heat ML strained 16% at 2150° F. As-polished, X1250 (reduced 29% on reproduction)

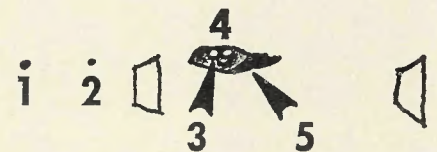


Fig. 2—Schematic drawing of regions in Fig. 1, analyzed by electron microprobe

Table 2—Sample Diffraction Data Observed with Weld Metal Residue of Heat MG

Observed diffraction line relative intensity ^a	d, Å	M ₆ C-type carbide ^b	ZrN 2-0956 ^c	Ni ₃ Si 3-0943 ^c	Calculated "expected" intensity
5	3.29			3.31 (4) 80	4
5	2.81			2.86 (3) 60	3
5	2.73	2.74 (8) 10		2.73 (4)	12
30	2.62		2.64 (30) 100		30
15	2.50	2.51 (16) 20			16
40	2.27		2.29 (30) 100	2.28 (5) 100	35
70	2.23	2.23 (64) 80			64
100	2.10	2.10 (80) 100		2.12 (3) 60	83

^a Intensities estimated visually.

^b Refers to reference 41.

^c Refers to card number in ASTM Powder Data File.

techniques for the selected areas. Where pulse-counting techniques were employed to arrive at concentrations, an estimate of the 50% confidence level is indicated, based upon the calculated values of the precision of measurement of the corresponding pulse counts.

The left-hand vertical column in Table 3 lists the nominal alloy composition and provides the best estimate of the composition of the cellular-dendritic matrix. Compare these data with the data shown in column 2 for the microconstituent identified as areas 1 and 2 in Fig. 2. Note that regions 1 and 2 were significantly depleted in Ni, Fe, Co and enriched in Cr, Mo, S, Si and Mn, with Mo and Si showing the most pronounced segregation. The positive segregation of S is definitely significant, while that of Mn is somewhat less so.

Since no point count was made for Cr in this constituent, the estimated Cr content shown was obtained from a material balance calculation. Despite this oversight, the positive segregation of Cr is believed to be significant.

The microprobe analysis of region 3 in Fig. 2 is summarized in column 3 of Table 3. Comparison of these data with those for the matrix (column 1) reveals that this grey area in Fig. 1 was slightly depleted in Ni, Fe, and Co. Of the remaining elements, Mo was most strongly segregated in this region, while Cr and Si were enriched to a slight degree. However, neither the S nor the Mn content of region 3 differed significantly from that of the matrix.

Region 4, the light spherical particle surrounded by region 3 was so located that the scans for Ni, Fe and Co apparently failed to intersect this constituent and no analyses of these elements was obtained. Again, Mo, Si and S appear to be segregated in this region, with Mo the most strongly segregated and Si the least. The Cr

Table 3—Results of Electron Microprobe Analysis of Fusion-Zone Microconstituents in a Specimen of Heat ML, Wt-%

	Nominal composition cell matrix	Regions 1 and 2 spherical particles	Region 3 grey constituent	Region 4 light particle	Region 5 dark constituent
Ni	48.56	38	44	N.A. ^a	33
Cr	21.88 ± 0.1 ^c	31 ^b	24.4 ± 0.1	25.1 ± 0.1 ^b	34 ^b
Fe	17.96	14	14	N.A. ^a	16
Mo	8.80	15	17.6	12	16
Co	1.48	1.0	1.0	N.A. ^a	1.0
S	0.011 ± 0.003 ^c	0.021 ± 0.003 ^c	0.013 ± 0.003 ^c	0.032 ± 0.001 ^c	N.A. ^a
Si	0.25 ± 0.03 ^c	0.58 ± 0.04 ^c	0.34 ± 0.03 ^c	0.43 ± 0.04 ^c	N.A. ^a
Mn	0.31 ± 0.003 ^c	0.34 ± 0.006 ^c	0.32 ± 0.006 ^c	0.34 ± 0.003 ^c	N.A. ^a

^a N.A. indicates analyses are not available.

^b Further comment to be found in text.

^c ± indicates 50% confidence level.

concentration shown for this region should be considered as a minimum value since it was obtained from a point count taken at the mutual interface between regions 3 and 4. The true value of the Cr concentration must therefore be greater than the reported value of 25.1% which represents a weighted average of the Cr content of regions 3 and 4.

The composition of region 5 in Fig. 2 is summarized in column 5 of Table 3. Comparison of these data with the nominal analysis of the alloy presented in column 1 indicates that this dark constituent is strongly depleted in its Ni content and slightly depleted in its content of both Fe and Co. Although no data for the S, Si, and Mn contents are available, this constituent is significantly enriched in both Mo and Cr. As was the case in regions 1 and 2, the concentration of Cr was deduced from a material balance calculation, and is believed indicative of the strong segregation of Cr.

Comparison of Fusion-Zone Microconstituents in Heats MK and ML

Figure 3 is a specimen current image taken at X750 of the fusion-zone microstructure in a sample of heat MK previously subjected to 14% strain at 2150° F. Figure 4 is a schematic drawing of this region with the areas of interest identified by number. Figure 5 is an optical micrograph of the same region taken at X750 showing the structure as revealed by electrolytic etching with 10% oxalic acid. The concentrations

of S, Si, and Mn detected by pulse counting at each selected location are presented in Table 4 together with the estimated 50% confidence level. Table 4 permits comparison of these data with similar data previously presented for comparable microconstituents in heat ML in Table 3.

Examination of these data reveals that similar segregation behavior occurs with respect to the partition of S, Si, and Mn in the fusion-zones of both heats MK and ML. Comparison of the data for both region 2 (white particles in Fig. 3) and region 3 (the dark constituent) with the nominal analyses of each element reveals that both constituents are markedly enriched in Mn as compared with the matrix. It should be noted that the nominal solute content strongly influences the magnitude of solute concentration observed in the various regions.

In all but one instance heat MK, with the higher nominal S, Si, and Mn contents, exhibited a higher concentration of these elements within the two microconstituents than did heat ML. Thus, the concentration of the minor elements S, Si, and Mn in the microconstituents present in the fu-



Fig. 3—Specimen current image of specimen of heat MK strained 14% at 2150° F. As-polished. X750 (reduced 28% on reproduction)

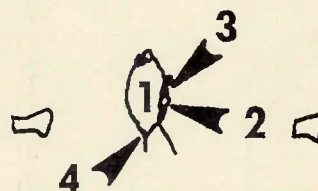


Fig. 4—Schematic drawing of regions in Fig. 3, analyzed by electron microprobe

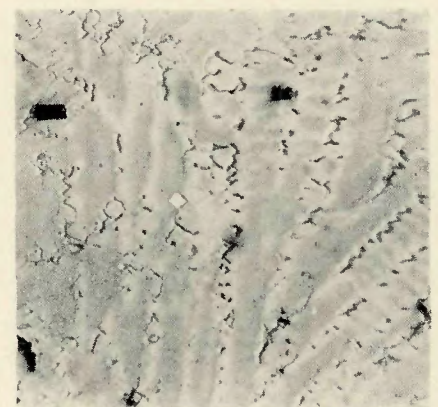


Fig. 5—Photomicrograph of area shown in Fig. 3, 10% oxalic acid electrolytic etch, X750 (reduced 31% on reproduction)

Table 4—Comparison of Minor Element Chemistry of Fusion-Zone Microconstituents in Heats MK and ML (Data on Heat ML were previously presented in Table 3)

Element	Heat	Region 1 cell matrix ^a	Region 2 white particle	Region 3 dark constituent	Region 4 sub-boundary triple point
S	MK	0.021 ± 0.003	0.086 ± 0.010	0.044 ± 0.006	0.023 ± 0.04
	ML	0.011 ± 0.003	0.032 ± 0.001	0.021 ± 0.003	N.A.
Si	MK	0.29 ± 0.04	0.49 ± 0.04	0.47 ± 0.04	0.34 ± 0.02
	ML	0.25 ± 0.03	0.43 ± 0.04	0.58 ± 0.04	N.A.
Mn	MK	0.93 ± 0.02	1.14 ± 0.02	1.06 ± 0.02	0.99 ± 0.03
	ML	0.31 ± 0.003	0.34 ± 0.003	0.34 ± 0.003	N.A.

^a Assumed to be the nominal analysis of each element.



Fig. 6—Specimen current image of a specimen of heat MK strained at 14% at 2150° F. As-polished, X750 (reduced 23% on reproduction)

sion-zone appears to increase roughly in proportion to the nominal amount of these elements. Since localized enrichment of S by a factor ranging from 2 to 4 was observed together with Si enrichment by a factor approaching 2, it is reasonable to expect that the melting temperature of these regions is significantly depressed with respect to that of the matrix. The extremely low hot-cracking resistance exhibited by heat MK during the testing portion of this investigation may, therefore, be attributed to the higher nominal composition of these minor elements.

An attempt was made to determine the degree of solute segregation at a sub-boundary triple point in the fusion-zone of heat MK. The data obtained are reported in column 4 of

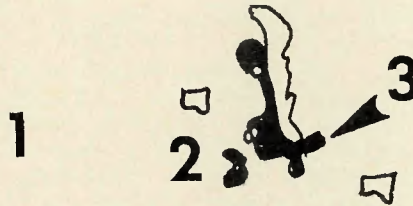


Fig. 7—Schematic drawing of regions in Fig. 6, analyzed by electron microprobe

Table 4 and do not indicate the presence of a significant degree of segregation. However it should be emphasized that in the absence of a distinct additional microconstituent, the width of such boundaries is below the theoretical resolving power of the microprobe. Therefore, considerable segregation could be present within the nominal width of the boundary without being detectable. In fact, the pronounced darkening of the subgrain boundaries in the specimen current image (Fig. 3) is evidence that such segregation actually exists.

Analysis of Selected Unidentified Heat-Affected Zone Microconstituents in Heat MK

Figure 6 is a specimen current image taken at X750 of the heat-affected zone microstructure of a sample of heat MK subjected to 14% strain at 2150° F. This particular region containing a microcrack was identified for analysis by the series of microhardness indentations visible as white trapezoidal shapes. Figure 7 is a

Table 5—Results of Electron Microprobe Analysis of Selected Unidentified Heat-Affected Zone Microconstituents in Heat MK, Wt-%

Element	Area 1 matrix ^a	Area 2 small constituent	Area 3 large constituent
Ni	47.17	28.5	32.4
Cr	22.21	30	24
Fe	18.16	14.5	12.6
Mo	8.80	23	30 (average)
Co	1.36	0.42	0.42
W	0.47	0.95	0.95
Si	0.29	0.53 ± 0.02	0.71 ± 0.03
Mn	0.93	0.67	0.67

^a Indicates matrix composition to be the nominal analysis.

schematic drawing of the region shown in Fig. 6 with the areas of interest identified by number.

Table 5 summarizes the analytical results obtained with the electron beam microprobe. Of the eight elements investigated, Mo is enriched by a factor ranging from 2.6 in area 2 to 3.3 in area 3 when compared with the nominal composition of the matrix. The level of Si increased by a factor of 1.8 in area 2 and 2.4 in area 3, thus experiencing the next most severe segregation. Of the other elements experiencing positive segregation, W was observed to have an enrichment factor of 2, while the Cr level was only slightly increased compared with the nominal composition.

The concentration of Ni, Fe, Co and Mn was reduced below the matrix composition in the two regions examined. The concentration of Co in both cases was approximately 1/3 of that found in the matrix, while that of Ni, Mn and Fe varied from 60 to 70% of the matrix concentration.

Analysis of Heat-Affected Zone Microconstituents (Previously Identified¹ by Metallographic Techniques)

Figure 8 shows a specimen current image taken at X1750 of the spherical η_2 - M_6C carbides and the eutectic constituent formed by interaction of the η_1 - M_6C carbides with the matrix in the heat-affected zone of an as-welded specimen of heat MK. This region is also shown in an optical photomicrograph in Fig. 9. The difference observed in the appearance of the microconstituents as shown in Figs. 8 and 9 are believed to result from intermediate polishing and etching operations.

The areas analyzed with the microprobe are identified by number in Fig. 8. Table 6 summarizes the results of the analyses conducted of these areas with the electron beam microprobe. The small, roughly spherical carbides in Fig. 9 are typically represented by areas identified as 1 in Fig. 8 and the analytical data are summarized in column 2. Note that the Mo content of this constituent is nearly 3.2 times that of the matrix. This is consistent with the identification of this phase as an M_6C carbide.⁷⁰⁻⁷² The silicon content in this area was found to be roughly twice that of the matrix while the remaining elements were observed to be depleted, except for S whose composition was unchanged. The concentration of Ni and Fe was reduced to 55-60% of the matrix level, while that of Mn was reduced to about 75%, and that of Cr approximated 90% of the nominal value.

Region 2, the white region in the

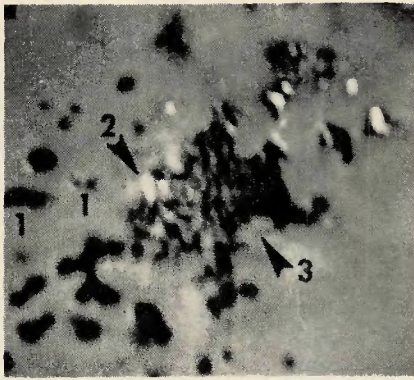


Fig. 8—Specimen current image of heat-affected zone microconstituents in as-welded specimen of heat MK. As-polished. X1750 (reduced 28% on reproduction)

specimen current image, exhibited an increase in Cr, Mo and S by a factor of 2 compared with the matrix composition. The Mn was increased by 30% in this area, while the Ni and Fe were decreased to approximately 60% of their respective concentrations observed in the matrix. Although conventional optical microscopy did not detect the existence of this region rich in S, Cr, Mo, and Mn, the results in Table 6 are consistent with the work of other investigators.⁵²

The average concentration in region 3, the eutectic constituent formed by the reaction between the η_1 -M₆C carbides and the matrix, discussed previously, is summarized in column 4 of Table 6. The Mo and Si contents of region 3 proved to be 2.5 and 2 times, respectively, the nominal content of the matrix.

Of the remaining elements, S showed no detectable segregation, while the Mn, Fe, Ni and Cr contents were less than the nominal level of these elements in the matrix.

X-Ray Analysis of Weld Metal Residues

Table 7 summarizes the compounds detected in the weld metal residues of the four heats studied. The 14 phases observed include 2 nitrides, 3 carbides, 6 sulfides, 2 intermetallic compounds, and a Ni-Fe solid solution.

The number of lines found in the four powder patterns ranged from

41-54 of which an average of 32 were located in the transmission region. Since the ASTM Powder Data Files for many compounds are incomplete for the back-reflection region, the identification of the compounds was based primarily upon the transmission lines. However, all existent back-reflection lines were checked once a compound was identified to ensure that no inconsistencies were present. In each powder pattern, all but one transmission line corresponding to a "d" spacing of 1.125 Å in Heat MJ and to 2.33 Å in heats MG, MK, and ML were accounted for by the compounds identified. In each pattern an average of 5 back-reflection lines could not be identified as a result of insufficient data for the back-reflection region of many compounds.

The X-ray fluorescence analysis of the weld metal residues obtained from all four heats confirmed the presence of all the major alloy elements (Ni, Cr, Fe, Mo, Co and W) and both Zr and Si. However, S and Mn were not detected probably as a result of the low atomic number in the case of S and the relatively small mass present in the case of Mn. Since no elements were detected by the fluorescence analyses that were not present in the list of compounds identified by X-ray diffraction, the fluorescence analysis provided indirect support of the X-ray diffraction results.

Relationship Between Hot-Cracking and Microstructural Features

The following sections summarize the role of individual microstructural features identified in the four heats of Hastelloy X studied on the formation of hot-cracks and microfissures. In general, phases or combinations of phases exhibiting a melting point or melting temperature range below that of the matrix phase are postulated to serve as sites for the nucleation of hot-cracks by the shrinkage strains associated with welding. Accordingly, each distinctive microstructural feature, whether identified by metallographic or X-ray techniques, will be considered separately and its possible role in hot-cracking assessed.

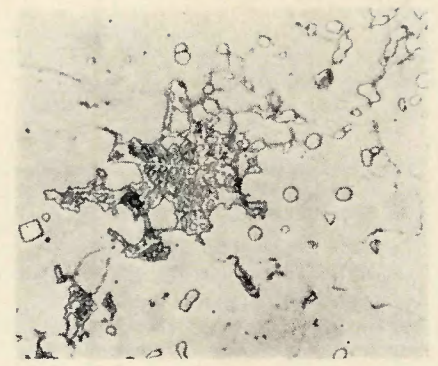


Fig. 9—Photomicrograph of area shown in Fig. 8. 10% oxalic acid electrolytic etch. X1500 (reduced 50% on reproduction)

Nitrides. Both ZrN and Cr₂N were positively identified from the diffraction patterns of the weld metal residues. ZrN was identified from the residue of all four heats studied, and this finding is in agreement with the results of metallographic studies previously discussed.¹ However, since this compound is reported to have a melting temperature of 2950° C (5342° F), its presence is not considered to be detrimental from the standpoint of hot-cracking or microfissuring. This is further supported by the metallographic studies which showed no detectable reaction between ZrN and the surrounding matrix either in the fusion-zone or the weld heat-affected zone. Furthermore, no evidence of micro-cracking associated with ZrN particles was observed in any of the test specimens examined metallographically.

The second nitride identified was of the form Cr₂N. Although this compound was not identified in the previous metallographic studies, its existence may be rationalized in terms of its high thermodynamic stability.⁷³⁻⁷⁵ This nitride was found in all heats except the low-nitrogen Heat ML which contained 454 ppm as con-

Table 6—Results of Electron Microprobe Analysis of Metallographically-Identified Heat-Affected Zone Microconstituents in Heat MK, Wt-%

Element	Nominal analysis	Region 1 spherical carbides	Region 2 white area	Region 3 large eutectic structure
Ni	47.17	26	26	37
Cr	22.21	20	41	20
Fe	18.16	11	11	14
Mo	8.80	28	17	22
S	0.021	0.021	0.042	0.021
Si	0.29	0.6	0.29	0.6
Mn	0.93	0.7	1.2	0.6

Table 7—Summary of Phases Detected by X-Ray Diffraction Analysis of Weld Metal Residues^a

Nitrides	Sulfides
ZrN	Co ₉ S ₄
Cr ₂ N	Cr ₃ S ₆
	Cr ₂ S ₄
	Fe _{x-1} S _x
Carbides	Miscellaneous
M ₆ C	M _n S
M ₂₃ C ₆	M _n S ₂
(Cr, Fe) ₇ C ₃	Co ₇ W ₆
	Ni ₃ Si
	(Ni, Fe) solid solution

^a A single, unidentified transmission line corresponding to a "d" spacing of 2.33Å was observed in the patterns of heats MG, MK, and ML; and a line, 1.125Å remained unidentified in the pattern of heat MJ.

trasted with an average of 816 ppm in heats MG, MJ, and MK (refer to Table 1). Although no definite data on the melting temperature of Cr_2N were found, the available thermodynamic data suggest that its melting temperature would be sufficiently high to preclude either melting or reaction with the surrounding matrix at the temperatures encountered in welding. Consequently, Cr_2N is not believed to contribute to the formation of hot-cracks or microfissures in Hastelloy X.

Carbides. The most abundant carbide identified in the residue was of the form M_6C . Although both the literature and the previous metallographic studies¹ indicate the existence of two distinct forms, η_1 - and η_2 - M_6C , the X-ray techniques employed were not sophisticated enough to resolve the small difference in the lattice parameter distinguishing these two forms. Thus, the metallographic techniques proved to be more suitable for differentiating η_1 from η_2 - M_6C than the X-ray diffraction techniques employed.

The metallographic studies indicated that the η_2 carbide was stable with respect to the matrix to a slightly higher temperature than the η_1 - M_6C carbide. In fact, the η_1 - M_6C may be seen to experience a form of constitutional liquation by reacting with the surrounding matrix at a temperature previously estimated¹ to be 2250° F. The typical eutectic produced by this reaction tended to produce isolated pools of liquid surrounding the original location of the carbide, and grain-boundary penetration was observed to emanate from these regions. Although no metallographic evidence of microcracks associated with the reaction of this carbide has been presented, examples of microcrack initiation were frequently observed metallographically during the conduct of the testing portion¹ of this program.

The more stable η_2 - M_6C carbide was observed to experience a reaction with the surrounding matrix at a slightly higher temperature, approximating 2300° F. The reaction product of the η_2 carbide and the matrix failed to develop the characteristic metallographic appearance of a eutectic constituent, but the pronounced tendency for this reaction product to penetrate adjacent grain-boundaries for a considerable distance supports the postulate that a liquid product formed. Evidence of hot-cracking associated with products of the reaction between η_2 carbide and the matrix was also commonly observed.

The X-ray diffraction studies of weld-metal residues demonstrated the

existence of both M_{23}C_6 and $(\text{Cr, Fe})_7\text{C}_3$. Although neither of these carbides was positively identified metallographically, it is probable that the smaller unidentified grain-boundary carbides found in the base metal of this alloy¹ consist of one or both of the above carbides. In the absence of positive metallographic identification, it was impossible to establish the temperature and type of reaction between either of these carbides and the matrix. However, it seems likely that matrix-carbide reactions similar to those observed for both M_6C -type carbides must occur in some characteristic temperature range. If, as reported in the literature,^{58, 76} the M_{23}C_6 and $(\text{Cr, Fe})_7\text{C}_3$ are preferentially located along grain-boundaries, these carbides could contribute a significant influence on the initiation and propagation of hot-cracks.

In general, the alloy carbides detected in Hastelloy X can contribute to the initiation of hot-cracks by reacting with the surrounding matrix to form a low-melting constituent which readily penetrates the grain-boundaries of the weld fusion-zone and weld heat-affected zone. Furthermore, it should be emphasized that the distribution of the carbides in the base-metal has an extremely important influence on their contribution to hot-cracking. In general, where alloy segregation, residual from the ingot phase, causes extensive segregation of carbides in banded patterns, the propensity for hot-cracking is greatly increased in the neighborhood of the carbide bands. This observation is clearly supported by metallographic examination of numerous test specimens.

Sulfides. The six sulfides identified from X-ray diffraction analysis include Co_3S_4 , Cr_5S_6 , Cr_7S_8 , MoS_2 , MnS , and $\text{Fe}_{x-1}\text{S}_x$. Although none of these sulfides could be positively identified from metallographic examination, present in all photomicrographs were additional unidentified constituents, some of which are undoubtedly sulfides from this group. All six of the above sulfides were found to be present in the residue of the high-S heat, MK, with a nominal S content of 0.021%. The remaining three heats with nominal S contents from 0.008 to 0.011% generally showed only 3 or 4 of the above six sulfides in their respective weld metal residues.

With regard to the role of sulfides, it is recognized that sulfides in general either exhibit low-melting temperatures or form in combination with other elements low-melting eutectic constituents. An extensive search of the literature failed to reveal data on

the melting temperatures of all of the sulfides. However, MoS_2 is reported⁷⁷ to have a melting temperature of 1185° C (2164° F) which corresponds closely to the temperature range at which hot-cracking was observed in the testing program. The melting point of MnS is reported as⁷⁸ 1600° C \pm 10° (2912° F) which is well above the melting range of Hastelloy X. However, eutectics between MnS and other elements present exhibit melting temperatures ranging upward from that of the Fe-Mn-S eutectic of 1000° C (1832° F).

Thus, the synergistic effect of the many components can materially alter the melting temperature of any of the sulfides present. Therefore, melting point data for the pure compounds would be of little significance anyway. It must be concluded that the presence of sulfides can contribute to the formation of hot cracks by providing a mechanism for localized depression of the melting temperature. Again, the distribution of the sulfides is extremely important in determining their contribution to the initiation and propagation of hot-cracks.

It is universally reported in the literature that sulfides and S-rich constituents are preferentially located along grain-boundaries where hot-crack initiation and propagation is observed. Thus, the hot-cracking propensity of an alloy can be related to the amount of sulfide present as it influences the continuity of the resulting low-melting grain-boundary constituent. This observation is supported by the higher cracking propensity of the high-S Heat MK as compared with the low-S Heat MJ with approximately the same level of other residuals.

Miscellaneous Microconstituents

Three additional microconstituents were identified by X-ray diffraction analysis. Of these, an intermetallic Co_7W_6 was positively identified, but examination of the Co-W constitutional diagram^{76, 78} reveals the solidus temperature in this range of composition to be 1465° C (2669° F). Thus it must be concluded that Co_7W_6 would not contribute to the proposed mechanism of hot-cracking, being solid to temperatures above the melting temperature range of Hastelloy X.

The second, Ni_2Si , also positively identified, is reported to have a melting temperature of 1319° C (2400° F).⁷⁸ Thus, in the absence of synergistic effects, this compound also would not be expected to contribute to the formation of hot-cracks. The composition of the third constituent, a

Ni-Fe solid solution is not tabulated in the ASTM Data File; however, the minimum value of the liquidus occurs at 1436° C (2617° F)⁷⁸ and therefore the melting temperature of any Ni-Fe solid solution can not be lower in the absence of synergistic effects.

Microsegregation

Unfortunately, the current resolution capability of the electron beam microprobe analyzer under ideal conditions is approximately one order of magnitude too low to permit quantitative analysis of the microsegregation associated with welding. In the weld fusion-zone the solidification mechanisms prevalent produce a network of solute-rich solidification subgrain-boundaries separated by distances averaging 10 microns. That these boundaries are solute-enriched can be clearly demonstrated both by conventional metallographic techniques and by specimen current image microscopy. Note that in Fig. 5 an optical photomicrograph, the etchant clearly reveals the location of the solidification subgrain-boundaries even in the absence of second-phases by a differential attack. Note also that in two typical specimen current images of the fusion-zone (refer to Figs. 1 and 37) the image density differs significantly along these subgrain boundaries, clearly establishing the existence of a compositional difference. However, all attempts to establish the magnitude of these compositional differences quantitatively, even by pulse-counting techniques, failed due to the magnitude of the effective volume fluoresced compared with the actual width of the solute-rich boundary. Thus, the microprobe analysis obtained by centering the beam on a typical subgrain- or grain-boundary represents a weighted average for a volume of which the actual solute-rich boundary is a negligibly small fraction.

Consequently, indirect qualitative methods, such as the utilization of selective etchants, provide the only sensitive means for detecting such microsegregation. However, in every instance in this and other investigations^{1-79, 80} hot cracks have been shown to initiate and propagate in these solute-rich regions under the influence of mechanical strain.

Therefore, it appears that the formation of hot-cracks can result both from the action of shrinkage strains upon localized low-melting regions whether produced by microsegregation during solidification, the presence of unfavorably distributed low-melting phases, or reactions between specific microconstituents and the surrounding matrix. In

any case, the presence of macro- and/or microsegregation in the original base metals must be considered as having a detrimental influence on the propensity for hot-cracking. Thus, it must be recognized that if a small-scale laboratory test for hot-cracking is to provide a satisfactory evaluation of weldability, the macro- and microsegregation present in the laboratory specimens must be truly representative of that present in the overall base metal as used in practice.

Conclusions

1. The following conclusions pertain to the electron microprobe analyses of the weld fusion-zone:

- (a) Specimen current images clearly indicated the presence of solute segregation within subgrain-boundaries whose dimensions were less than the resolution limit of the microprobe analyzer.
- (b) The presence of subgrain- and grain-boundary micro-constituents confirmed that significant segregation of solute occurs during the solidification of a weld.
- (c) The differing appearance of three microconstituents shown in the electron-image micrographs of fusion-zone structures indicated the existence of several different types of compounds present in the fusion-zones of both heats MK and ML.
- (d) Relative to the matrix analysis (assumed to be representative of the nominal) the subgrain- and grain-boundary microconstituents were highly enriched in Mo, S, and Si; only slightly enriched in both Cr and Mn; and significantly depleted in Ni, Fe, and Co.
- (e) The concentrations of S, Si, and Mn, when observed in comparable microconstituents found in both heats MK and ML, were shown to be higher in heat MK (0.021 S—0.29 Si—0.93 Mn) than in heat ML (0.011 S—0.25 Si—0.31 Mn).

2. The following conclusions pertain to the electron microprobe analysis of heat-affected zone microconstituents:

- (a) Regions, not detectable by conventional optical microscopy, were observed by specimen current-image techniques and were shown to be enriched significantly in Cr, S, Si, Mn, and Mo.
- (b) Both the η_1 - and η_2 M₆C carbides exhibited significantly higher concentrations of Mo, S, and Si; a slightly depleted concentration of Mn, and considerably lower contents of Cr, Ni, and Fe when compared to those in the matrix.
- (c) Grain-boundary constituents, metallographically observed but unidentified, were strongly enriched in Mo, W, S, and Si; slightly en-

riched in Cr; and significantly depleted in Ni, Fe, Co, and Mn.

3. The following conclusions pertain to the compounds identified in the weld metal residues and their respective importance to hot-cracking in Hastelloy X:

- (a) Fourteen phases were detected in the weld metal residues, including two nitrides (ZrN, Cr₂N); three carbides (M₆C, M₂₃C₆, (Cr, Fe)₇C₃); six sulfides (Co₃S₄, Cr₆S₆, Cr₇S₈, Fe_{x-1}S_x, MnS, MoS₂), and three miscellaneous constituents (Co₇W₆, Ni₂Si, Ni-Fe solid solution).
- (b) Because of their high melting temperature ranges, the ZrN, Cr₂N, Co₇W₆, Ni₂Si, and (Ni, Fe) phases present were considered to have no influence on hot-cracking in Hastelloy X without synergistic effects.
- (c) The carbide phases were observed to provide easy nucleation sites for hot-cracks by the mechanism of constitutional liquation.
- (d) The sulfide phases are considered detrimental to the hot-cracking resistance of Hastelloy X, and are believed to be the cause of the poor hot-cracking behavior shown by the S-rich heat MK.

Acknowledgments

Thanks are due to Mr. Ernest S. Malizie of the Union Carbide Mining and Metals Division, Niagara Falls, N.Y. for his aid in performing the electron microprobe analyses, to Mr. John Hatheway of the General Electric Silicone Products Department, Watertown, N.Y. for his aid in performing the X-ray fluorescence analyses, and to Mr. Lou Osika of the General Electric Research and Development Center, Schenectady, N.Y. for making his X-ray diffraction laboratory facilities available to the authors.

The authors also extend their appreciation to Messrs. W. D. Manly, B. R. Barrett, W. Witting, and D. W. Schulz all of whom were at that time associated with the Union Carbide Stellite Division (now a division of the Cabot Corporation) for their kindness and willing advice, and to that division for its financial support of this investigation.

References

1. Savage, W. F., and Krantz, B. M., "An Investigation of Hot Cracking in Hastelloy X", WELDING JOURNAL, 45 (1) Research Suppl., 13-s to 25-s (1966).
2. Pfann, W. G., "Zone Melting," John Wiley, New York, 1950.
3. Smith, V. G., et al. Can. J. Physics, 33, 723 (1955).
4. Weinberg, F., "Solute Segregation During Dendritic Growth," Trans AIME, 221 (8), 844-50 (1961).
5. Kattamis, T. Z., and Flemings, M. C.,

- "Dendrite Morphology, Microsegregation, and Homogenization of Low-Alloy Steel," *Trans AIME*, 223 (5), 992-99 (1965).
6. Ward, R. G., "The Dendritic Segregation of Mn in Steel Ingots," *J. Iron and Steel Institute*, 188 (4) 337-42 (1958).
7. Smeltzer, C. E., "Solve Steel 'Freckle' Mystery," *The Iron Age*, 184 (11), 188-89, Sept. 10, 1959.
8. Gould, G. C., "Freckle Segregation in Vacuum Consumable-Electrode Ingots," *Trans AIME*, 233 (7), 1345-51 (1965).
9. "Determination of Causes of Cracking in Welding Age-Hardenable High-Temperature Alloys," Tech. Documentary Report No. ASD TR61-678.
10. Gregg, R. A., and Pearcey, B. J., "Solute Distribution and Eutectic Formation in As-Cast Nickel-Base Superalloys," *Trans-AIME*, 230 (4), 599-600 (1964).
11. Beattie, H. J., Jr., and Ver Snyder, F. L., "Microconstituents in High-Temperature Alloys," *Trans ASM*, 45, 397-423 (1953).
12. Rollason, E. C., and Bystran, M. C. T., "Hot Cracking of Austenitic Welds," *J.I.S.I.*, 169, No. III, 347-52 (1951).
13. Brockhurst, P. J., and Muir, H., "Hot Cracking," *J. Australian Inst. Metals*, 10 (2), 140-48 (1965).
14. Sopher, R. P., et al., "Investigation of Weld-Metal Cracking in High-Strength Steel," *WELDING JOURNAL*, 34 (11), Research Suppl., 544-s to 552-s (1955).
15. Medovar, B. I., and Latash, Y. V., "All-Austenite Welds Not Susceptible to Hot Cracking," *Automaticheskaya Svarka*, 10 (2), 32-45 (1957).
16. Hoerl, A., and Moore, T. J., "The Welding of Type 347 Steels," *WELDING JOURNAL*, 36 (10), Research Suppl., 442-s to 448-s (1957).
17. Randall, M. D., et al., "Causes of Microcracking and Microporosity in Ultra-High Strength Steel Weld-Metal," *Ibid.*, 41 (5), Research Suppl., 193-s to 206-s (1962).
18. Rozet, D., et al., "Effect of Weld Metal Composition on the Strength and Ductility of 15% Cr-35% Ni Welds," *Ibid.*, 27, Research Suppl., 481-s to 491-s (1948).
19. Lyubavskii, K. V., and Toropov, V. A., *Paton Commemoration Volume*, Mashgiz, 117-34 (1956).
20. Borland, J. C., "Suggested Explanation of Hot Cracking in Mild and Low Alloy Steel Welds," *Brit. Welding Journal*, 3, 526 (1961).
21. Pease, G. R., "The Practical Welding Metallurgy of Nickel and High-Nickel Alloys," *WELDING JOURNAL*, 36 (7), Research Suppl., 330-s to 334-s (1957).
22. Linnert, G. E., and Bloom F. K., Discussion in *WELDING JOURNAL*, 26 (2), Research Suppl., 119-s to 120-s (1947).
23. Avakyan, S. V., and Lashko, N. F., "Primary Structure and Causes of Weld Hot-Cracking of Chromansil-Type Steel," *Autogennoe Delo*, 21 (10), 13-16 (1950).
24. Medovar, B. I., *Auto. Svarka*, 6, 3-23 (1952).
25. Goldschmidt, H. J., Discussion in *J.I.S.I.*, 337-44 (1952).
26. Linnert, G. E., "Welding Type 347 Stainless Steel Piping and Tubing," *Welding Research Council Bulletin* No. 43, October 1958.
27. Medovar, B. I., "Effect of Solubility of Alloying Elements on Hot Cracking," *Auto. Svarka*, 7 (4), 12-28 (1954). Henry Brucher Translation #3554.
28. Medovar, B. I., *Paton Commemoration Volume*, Mashgiz, 150-61 (1956).
29. Personal Communication, Richman, M., Universal-Cyclops Specialty Steel Corp., Bridgeville, Pennsylvania. (1965).
30. Podgaetskii, V. V., "Reasons for Hot Cracking of Welds," *Auto. Svarka*, 7 (6), 73-76 (1954). Henry Brucher Translation #3536.
31. Van Vlack, L. H. et al., "Sulfide Inclusions in Steel," *Trans AIME*, 221, 220-28 (1961).
32. Silverman, E. N., "Synthetic Inclusions in the FeO-MnO-MnS-SiO₂ System in Equilibrium with Resulfurized Steel," *Trans AIME*, 221 (3), 512-17 (1961).
33. Owczarski, W. A., and Sullivan, C. P., "Effect of Postweld Heat Treatment on a Superalloy Weld Deposit," *WELDING JOURNAL*, 44 (6), Research Suppl., 241-s to 250-s (1965).
34. Cordea, J. N. et al., "Causes of Fissuring in Nickel-Base and Stainless Steel Alloy Weld Metal," *Ibid.*, 43 (11), Research Suppl., 481-s to 491-s (1964).
35. Toropov, V. A., *Metallovedenie i obrabotka metallov*, 2, 45-50 (1956).
36. Heuschkel, J., "Initial Characteristics of Chromium-Nickel Steel Weld Metal," *WELDING JOURNAL*, 34, Research Suppl., 184-s to 504-s (1955).
37. Kauhausen, E., and Kautz, H. R., "Welding of Creep-Resisting Austenitic Materials," *British Welding Journal*, 9 (5), 266-79 (1962).
38. Bishop, E. S., and Bailey, W. H., Symposium of High Temperature Steels and Alloys, *Iron and Steel Inst.*, 225-32 (1952).
39. Boniszewski, T., and Baker, R. G., "Burning and Hot-Tearing in the Weld Heat-Affected-Zone of Ferritic Steel," *J.I.S.I.*, 202 (11), 921-29 (1964).
40. Brammer, E. S., et al., "A New Type of Grain Boundary Precipitate Observed in Cast Steel," *Acta Met.*, 6 (2), 134-5 (1958).
41. "Identification of Microconstituents in Superalloys", D.M.I.C. Memorandum #160, Battelle Memorial Institute, Columbus, Ohio.
42. Slaughter, G. M., et al., "Welding of Nickel-Molybdenum Alloys," *WELDING JOURNAL*, 38 (10), Research Suppl., 393-s to 400-s (1959).
43. Carey, J. D., and McKittrick, G. F., "Control of Fissuring in Inconel by Regulating Process Variables," *Ibid.*, 27 (12), Research Suppl., 529-s to 533-s (1962).
44. Kaufman, M., and Palty, A. E., "The Phase Structure of Inconel 718 and 702 Alloys," *Trans AIME*, 221 (12), 1253-62 (1961).
45. Westbrook, J. H., "Segregation at Grain Boundaries", Report No. 64-RL-3808M, General Electric Research and Development Center, Schenectady, N.Y., December, 1964. (217 References).
46. Owczarski, W. A., and Duvall, D. S., "Behavior of Solute at Mobile Heat-Affected-Zone Grain Boundaries", *WELDING JOURNAL*, 45 (8), Research Suppl., 356-s and 384-s (1966).
47. Kirk, D., and Cockcroft, M. G., "Ghost Boundaries as Markers in Copper", *J. Inst. Metals*, 88, 320 (1960).
48. Phillips, W. L., "Ghost Grain Boundaries as Markers in Nickel," *J. Inst. Metals*, 92, 94 (1963).
49. Masubuchi, K., and Martin, D. C., "Mechanisms of Cracking in HY-80 Steel Weldments", *WELDING JOURNAL*, 41 (8), Research Suppl., 375-s to 384-s (1962).
50. Brammar, I. S., "A New Examination of the Phenomena of Overheating and Burning of Steels", *J.I.S.I.*, 201 (9), 752-61 (1963).
51. Brammar, I. S., and Honeycombe, R. W. K., "Formation of Sulfides at Grain Boundaries in Some Pure Iron Alloys", *J.I.S.I.*, 202 (4), 335-42 (1964).
52. Kiessling, R., and Lange, N., Discussion in *J.I.S.I.*, 201 (9), 761-62 (1963). Original data reported in *J.I.S.I.*, 200, 914-21 (1962).
53. Brammar, I. S., and Honeycombe, R. W. K., (Authors' Reply to Discussion), *J.I.S.I.*, 201 (9), 762 (1963).
54. Kiessling, R., and Westerman, C., "Sulfide Inclusions and Synthetic Sulfides of the (Mn, Me) S-type," *J.I.S.I.*, 203 (4), 377-379 (1966).
55. Toropov, V. A., "Role of the Grain Boundary Substance in the Hot Cracking of Austenitic Welds", *Metallovedenie i Obrabotka Metallov*, 2 (4), 45-50 (1956).
- Henry Brucher Translation #3809.
56. Puzak, P. P., and Rischall, H., "Further Studies on Stainless Steel Hot Cracking," *WELDING JOURNAL*, 36 (2), Research Suppl., 57-s to 61-s (1957).
57. Personal Communication, R. G. Gilliland, Oak Ridge Laboratory, Oak Ridge, Tenn. (1965).
58. Stickler, R., and Vinekier, A., "Precipitation of Chromium Carbide on Grain Boundaries in a 302 Austenitic Stainless Steel", *Trans AIME*, 224 (10), 1021-24 (1962).
59. Smith, J. T., and Spencer, C. W., "Grain Growth in the Presence of an Intergranular Liquid", *Trans AIME*, 227 (6), 783-84 (1963).
60. Dudley, R. H., "An Experimental Investigation of the Constitutional Liquefaction Hypothesis", Ph.D. Thesis, Rensselaer Polytechnic Institute, January, 1962.
61. Aronson, A. H., "Constitutional Liquefaction in the Iron-Iron Carbide System", Master's Thesis, Rensselaer Polytechnic Institute, May 1963.
62. Owczarski, W. A., and Sullivan, C. P., "A Microstructure Study in a Welded Superalloy", *WELDING JOURNAL*, 43 (9), 393-s to 399-s (1964).
63. Sullivan, C. P., "Formation of a Eutectic Structure in the Heat-Affected-Zone of Udimet 700 Welds", *Trans ASM*, 57 (2), 572-75 (1964).
64. Owczarski, W. A., et al., "A Model for Heat-Affected-Zone Cracking in Nickel-Base Superalloys", *WELDING JOURNAL*, 45 (4), 145-s to 155-s (1966).
65. Pepe, J. J., and Savage, W. F., "The Weld Heat-Affected-Zone of the 18-Ni Maraging Steels", *WELDING JOURNAL*, 49 (12), Research Suppl., 545-s to 553-s (1970).
66. Cullity, B. D., "Elements of X-Ray Diffraction", Addison-Wesley, Reading, Mass. 1956.
67. Lane, J. R., and Grant, N. J., "Carbide Reactions in High-Temperature Alloys", *Trans ASM*, 44, 113-34 (1952).
68. Personal Communication, Mr. Lou Osika, Research and Development Center, General Electric Company, Schenectady, N.Y. (1960).
69. N. P. Pies, 969 Skyline Drive, Laguna Beach, California, 92651.
70. Beattie, H. J., Jr., and Ver Snyder, F. L., "Microconstituents in High-Temperature Alloys", *Trans ASM*, 45, 397-423 (1953).
71. Lund, C. H., "Physical Metallurgy of Nickel-Base Superalloys", D.M.I.C. Report 153, May 5, 1961, Battelle Memorial Institute, Columbus, Ohio.
72. Wilde, R. F., and Grant, N. J., "Aging in Complex Commercial Ni-Cr Alloys Hardened with Titanium and Aluminum", *Trans AIME*, 209 (7), 865-72 (1957).
73. Kubaschewski, O., and Evans, E. L., "Metallurgical Thermochemistry", Pergamon Press, London (1958).
74. Elliot, J. F., and Gleiser, M., "Thermochemistry for Steelmaking", Vol. I, Addison-Wesley, Reading, Mass. (1960).
75. Pearson, J., and Ende, V. J. C., "The Thermodynamics of Metal Nitrides and of Nitrogen in Iron and Steel", *J.I.S.I.*, 175, 52-58 (1953).
76. Weeton, J. W., and Signorelli, R. A., "Effect of Heat Treatment Upon Microstructures, Microconstituents, and Hardness of a Wrought Cobalt-Base Alloy", *Trans ASM*, 47, 815-845 (1955).
77. "Handbook of Chemistry and Physics", 36th Edition, Chemical Rubber Publishing Co., Cleveland (1954).
78. "Metals Handbook", 1948 Edition, A.S.M., Cleveland (1948).
79. Savage, W. F., and Lundin, C. D., "The Vrestraint Test", *WELDING JOURNAL*, 44 (10), Research Suppl., 433-s to 442-s (1965).
80. Unpublished work, Welding Laboratory, Rensselaer Polytechnic Institute, Troy, New York.

Authors . . . See pages 401 and 402 of the June 1971 WELDING JOURNAL if you wish to participate in the AWS 53rd Annual Meeting of the American Welding Society.